

SEISMIC PERFORMANCE OF A STEEL MOMENT-RESISTING FRAME SUBJECT TO STRENGTH AND DUCTILITY UNCERTAINTY*

A. K. Kazantzi,^{1†} D. Vamvatsikos², D. G. Lignos³

¹ J.B. ATE, Herakleion, Crete, Greece.

² School of Civil Engineering, National Technical University of Athens, Athens, Greece.

³ Department of Civil Engineering and Applied Mechanics, McGill University, Montreal, Canada.

Keywords: fragility; seismic performance; uncertainty; incremental dynamic analysis; demand-capacity correlation

***Abstract.** The reliable estimation of the seismic performance of structures requires quantifying the aleatory and epistemic uncertainties of the system parameters. This is efficiently achieved for a case study of a four-story steel moment-resisting frame through several important advances. First, a state-of-the-art numerical model is formed with full spatial parameterization of its strength and plastic deformation properties. Empirical relationships derived from experimental data are used to model the cyclic behavior of steel sections using probabilistically distributed parameters that include intra- and inter-component correlation. Finally, incremental dynamic analysis and Monte Carlo simulation are employed to accurately assess the seismic performance of the model under the influence of uncertainties. Of interest is the extent to which model parameter uncertainties may trigger negative demand-capacity correlation in structural fragility evaluation, where, for example, a lower ductility capacity for a component may decrease the threshold for local failure while at the same time raising the local demand estimate from an uncertainty-aware model. With respect to the examined steel moment-resisting frame and considering three construction quality levels (i.e. very good, average, low) as per FEMA P-58, it is shown that, despite the good agreement of the evaluated structural demands obtained with and without consideration of the model parameter uncertainties for well-designed modern buildings, the potential demand-capacity correlation is likely to give rise to unconservative estimates of fragility for local damage-states, especially in cases where substandard quality control is exercised during construction.*

1 INTRODUCTION

Several uncertainty sources come into play whenever an engineer attempts to assess the seismic performance of a structural system. They may be broadly organized into two main categories, these being the aleatory and the epistemic [1]. Aleatory uncertainties are associated with inherently random factors, such as the earthquake loading, and hence cannot be controlled. By contrast, epistemic uncertainty sources are related to our incomplete knowledge and can be potentially reduced, e.g., by employing testing to determine material properties or using more sophisticated numerical models and methods of analysis.

Up until now, several recent studies (e.g. [2; 3]) have concluded that the earthquake “signature” is the dominant uncertainty source. However, current research has, so far, only partially addressed the issue of the uncertainties related to the parameters of the structural

* Based on a short paper presented at the 11th International Conference on Structural Safety and Reliability (ICOSSAR 2013), New York, 2013.

† Corresponding author: kazantzi@mail.ntua.gr

model in seismic performance assessment (e.g. [4; 5; 6; 7; 8; 9; 10; 11]). For instance, Ibarra & Krawinkler [10] have shown that the model parameter uncertainties can have a significant impact on the predicted collapse performance when considering deteriorating hysteretic models. Nevertheless, the study is limited to single-degree-of-freedom (SDOF) systems and hence the validity of the outcomes to multi-degree-of-freedom (MDOF) systems is questionable. By contrast, Liel et al [6] investigated the model uncertainty significance for a set of reinforced concrete structures that were efficiently modeled to account for cyclic deterioration in flexural strength. This study concluded that neglecting the modeling uncertainties reduces the dispersion in the response fragility and also shifts the median predictions. Despite the revealing findings of this study, these are bounded to errors associated with the approximate nature of the response surface methodology. The latter was adopted for predicting the median collapse capacity as a function of the model random variables. On a different track, Vamvatsikos & Fragiadakis [9] investigated the model uncertainty effects on a steel moment-resisting frame (SMRF) by means of Monte Carlo simulation paired with Latin Hypercube Sampling. The study concluded that the model parameter uncertainties can have an important contribution to the overall response dispersion. Yet, generalization of the findings is limited due to the fact that the probabilistic modeling of the uncertain parameters was not founded on experimental data.

In fact, with respect to the deterioration modeling of steel frames, only limited research (e.g. [9; 12; 13; 14]) has been focused explicitly on the model parameter uncertainty in the structural component capacity. However, even in these studies, deterioration modeling was based either on expert opinion or on empirical expressions derived from small experimental databases, using simplified assumptions to employ the best possible capacity estimates given the limited available data. To this end, the dependence of the models proposed by e.g. FEMA 355D [15], Mele [16] and Kazantzi et al [14] for estimating the steel component capacities on a single structural property (i.e. the beam depth), may be considered a step forward. Nevertheless, they have left ample space for more elaborate research towards enhanced steel structural modeling and capacity uncertainty consideration. On account of the above, relatively recently, Lignos & Krawinkler [17] provided detailed relationships for modeling the cyclic deterioration in flexural strength and stiffness of structural steel components [18]. The proposed multi-variable empirical equations allow the prediction of several modeling parameters on the basis of more than 300 steel wide flange beam experiments.

Furthermore, all pertinent studies have been confined so far to a full spatial correlation assumption, meaning that parameter changes are effected uniformly throughout a building, vastly reducing the dimensionality of the problem but at the same time exaggerating its sensitivity to model parameters. Thus, it can be inferred that the holistic quantification of the model parameter uncertainties and how these propagate into the analysis and performance predictions remains an open issue.

Aiming to provide such an outlook this research attempts to quantify the model parameter uncertainty for a case study of a well-designed contemporary four-story SMRF, considering three levels of construction quality (i.e. very good, average and low). To efficiently reduce the complexity of the problem, following the findings of Fragiadakis et al [19], mass and stiffness parameters are considered deterministic (as they contribute the least to structural performance variability) while the strength and ductility properties of the components are fully parameterized. The empirical relationships derived from experimental data and recently proposed by Lignos & Krawinkler [17] are used to model the cyclic behavior of steel components via parameters that determine the pre- and post-capping plastic rotation, the cyclic deterioration in flexural strength and stiffness, the effective yield strength and the post-yield strength ratio of steel components subjected to cyclic loading. Such variables are completely described at the local level by probabilistic distributions that incorporate intra-

component and inter-component correlation information throughout the entire structure. The magnitude of component uncertainties, are calibrated to correspond to three construction quality levels considering the dispersion estimates proposed by Lignos & Krawinkler [17] and the recommendations of FEMA P-58-1 [20] to account for differing levels of quality control. Incremental dynamic analysis [21] is employed to accurately assess the seismic performance of the model, for any combination of the parameters in tandem with an efficient Monte Carlo simulation algorithm based on record-wise incremental Latin Hypercube Sampling (LHS) to propagate the uncertainties from the model parameters to the actual system demand and capacity [22].

Our aim is twofold. First, we seek to quantify the effect of realistic parameter uncertainties on structural response and extract default dispersion values to be used for performance assessment of regular low-rise capacity-designed SMRFs at different levels of construction quality control. Second, we shall investigate the effect of the demand-capacity (DC) correlation on the fragility estimation. The DC correlation accounts for the intuitive fact that component properties tie together the model response and the component fragility, in the sense that for instance, lower component capacities in a structural model may result to higher demands and consequently lead to a left-shifted fragility function. While its existence has been suggested by Cornell et al [23], given that this potential source of bias is typically ignored even in the most advanced seismic performance assessment guidelines (e.g. FEMA P-58-1 [20]) it becomes important to map its effect and potential consequences for loss calculations.

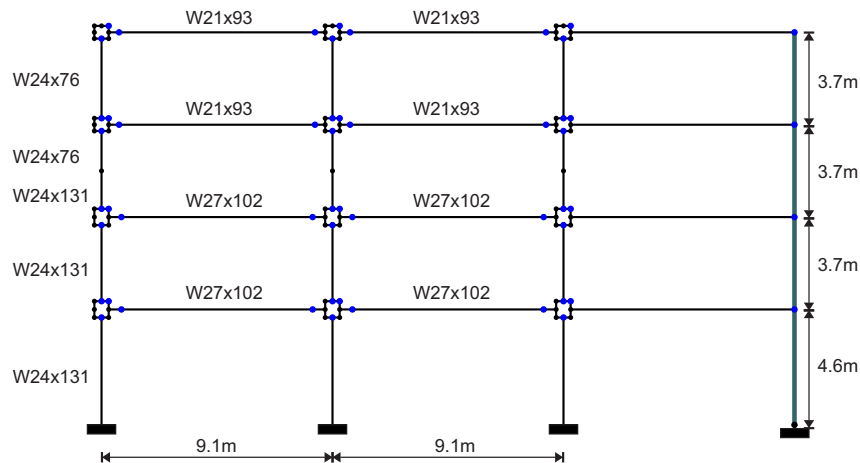


Figure 1. 2D model idealization with leaning column of the analyzed East-West MRF.

2 ANALYTICAL MODELING

2.1 Structural model

The effect of the model parameter uncertainties on the seismic performance will be quantified by means of a case study steel moment-resisting frame building. The building consists of four stories, the first being 4.6m (15ft) high and the ones above 3.7m (12ft). It was designed as an office building to 2003 IBC [24] and AISC [25] for the Los Angeles area and it has a rectangular floor plan consisting of 3 bays at 9.1m (30ft) in the North-South direction and 4 bays at 9.1m (30ft) in the East-West direction. Our focus will be the East-West framing, in which only the two middle bays are moment-resisting. The columns of the moment-resisting bays were assumed to be fixed at their bases, whereas they are also spliced at the mid-height of the third story. The beams were designed as reduced sections (RBS) with their

‘dogbone’ geometries detailed according to FEMA 350 [26]. The moment-resisting frames (MRFs) are also capacity-designed, implying that the final steel section sizes satisfy the AISC strong column-weak beam requirement.

The building’s seismic performance was evaluated using a 2D analytical model with elastic elements in OpenSees [27] where plastic hinge formation (point plasticity) was allowed at column ends as well as at the ‘dogbone’ location for beams. The stiffness of the rotational springs used to represent the point hinges was set to be 10 times larger than that of the associated element as shown in Ibarra and Krawinkler [10]. P- Δ effects were included using a first-order treatment of geometric nonlinearity. In addition, a leaning column was added to account for the destabilizing effect of the gravity frame loads without axially stressing the lateral load resisting columns. Furthermore, the mathematical idealization of the frame includes shear deformation due to panel zones by means of a model proposed by Krawinkler (see [28] for a detailed description), which uses a set of rigid links to form a parallelogram. The shear strength and stiffness of the panel zone is depicted by a trilinear rotational spring, which for the case at hand is located at the upper right corner of the parallelogram (see Figure 1). In addition, due to limitations related to the adopted analytical model, the interaction between moment and axial force was disregarded at column elements. This however, is anticipated to have only minor effect on the column strengths of the considered capacity-designed steel MRF, given that plastic hinging at low to moderate drift levels in such buildings is concentrated mainly at beam ends. Hence, local damage levels are unlikely to be affected by such simplification. The first three vibration periods of the analyzed frame were found to be 1.33, 0.40 and 0.19sec, whereas 2% Rayleigh damping was assumed at the first and third mode of vibration. Figure 1 depicts the 2-D model used for the East-West MRF along with the beam and column section sizes. Additional details regarding the frame configuration, design and idealization can be found in Lignos et al [29].

2.2 Probabilistic model

As discussed, the probabilistic model of the four-story structure contains a full spatial description of member strength and ductility properties, while assuming deterministic mass, stiffness and damping, due to documented expectations for their lower significance [e.g. 19]. For a moment-resisting frame modeled using lumped plasticity elements, this effort essentially culminates to the description of each of the beam and column plastic hinge properties. The rotational springs at the member ends (or ‘dogbone’ location for beams) are idealized by the Ibarra-Medina-Krawinkler (IMK) model [30] as this was modified by Lignos and Krawinkler [31] to incorporate asymmetric component hysteretic behavior as well as ultimate deformation rotation. This model was implemented in the OpenSees open-source analysis platform [27]. As shown in Figure 2, it entails five parameters per hinge that completely account for the nonlinearity in the model, namely (a) the pre-capping (i.e., pre-maximum moment) plastic rotation θ_p , (b) the post-capping (i.e. from maximum moment to fracture) plastic rotation θ_{pc} , (c) the cumulative rotation capacity Λ that determines the reference energy dissipation capacity of a structural component, (d) the ratio of effective (actual) to estimated yield-strength $M_y/M_{y,p}$ and (e) the post-yield (maximum) strength ratio M_c/M_y . In total, for 20 members times two plastic hinges each, the four-story SMRF becomes a 200 random variable model. It should be pointed out that Figure 2 is meant to represent two potential instances of a generic moment-rotation relationship. The actual member moment-rotation curve either follows the solid line exclusively or deviates onto the dotted one, depending on the end point. Whichever endpoint (zero-strength rotation) is reached first determines the branch that the moment-rotation relationship will follow.

To determine their properties, Lignos & Krawinkler [17] have fitted a comprehensive database of structural tests using regression equations that incorporate the effect of material,

section geometry and member dimensions. This database is available from the following link: <http://dimitrios-lignos.research.mcgill.ca/databases/>. Results are offered separately for beams with RBS ends and beams other-than-RBS. The former will be employed for beams and the latter, for lack of better data, to model the columns. For the first three parameters, i.e., θ_p , θ_{pc} , Λ the lognormal distribution was found to fit the experimental data satisfactorily, while for $M_y/M_{y,p}$ and M_c/M_y a normal distribution is recommended.

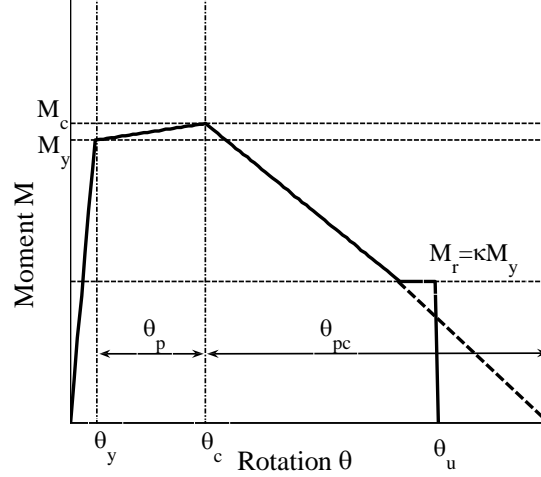


Figure 2. Monotonic moment-rotation relationship for the modified IMK deterioration model (adopted from [17]).

Along with the proposed median values, evaluated using an expected yield strength $f_y=379\text{MPa}$ (55ksi), Lignos & Krawinkler [17] also provided the dispersion of the lognormally (i.e. θ_p , θ_{pc} , Λ) and the normally (i.e. $M_y/M_{y,p}$ and M_c/M_y) distributed data. These dispersion estimates are summarized in Table 2 and can be considered to reflect ‘good’ construction practices, since all the tested specimens used for regression were prepared in controlled laboratory conditions. It is worth pointing out that a direct comparison of these values to those reported elsewhere should be undertaken with caution since, for example, neither the reference energy dissipation capacity Λ nor the post-capping plastic rotation θ_{pc} can be strictly paired with a distinct limit state, such as those provided by FEMA P-58-1 [20].

In particular, FEMA P-58 decomposes the total dispersion β of a damage-state engineering demand parameter (EDP)-value of capacity, to three main ingredients, these being the uncertainty in the design/prediction equation for the parameters β_D , the material uncertainty β_M and the construction quality uncertainty β_C . On account of the above, the total uncertainty β can be computed as,

$$\beta = \sqrt{\beta_D^2 + \beta_M^2 + \beta_C^2 + \beta_{\min}^2} \leq \beta_{\max} \quad (1)$$

with $\beta_{\min} = 0$ and $\beta_{\max} = 0.5$ for strength-limited states versus $\beta_{\min} = 0.4$ and $\beta_{\max} = 0.6$ for ductility-limited ones. No adjustment to the central value (mean or median) of the fragility/parameter distributions is employed, implicitly assuming that even lower quality control standards do not generate a consistent bias in the quality of the connections. Simply put, when considering all the potential realizations of the SMRF, connections are assumed to be equally likely to be better or worse than their ‘central value’, rather than, say, consistently badly executed. Of course, some possible SMRF realizations will come off with all connections on the minus side (e.g., performed by a single sloppy crew), but they will be balanced in the overall ensemble by other SMRF realizations that are on the plus side. Thus, lower quality standards will only introduce noise, rather than consistently worse-than-

expected behavior. The effects of the latter are not too difficult to imagine and they are not the subject of this study.

Since FEMA P-58-1 [20] recommendations are linked to component damage-states rather than component parameters per se, each of the five hinge parameters was assigned to one of three generic damage-state (or failure mode) types as per FEMA P-58:

- a) Ductile, simple behavior: This refers to damage-states that are well-predicted by classical mechanics and have a low sensitivity to construction quality, essentially, any parameter related to yielding and to the maximum (capping) strength of steel sections (but not their ductility). It concerns parameters $M_y/M_{y,p}$ and M_c/M_y , both considered to be strength-limited parameters, i.e. using the lower values of β_{min} and β_{max} in Eq. (1).
- b) Ductile, complex behavior: Damage-states where ductility still provides a margin of safety but predictive equations are not readily available, are inherently indicative of complex nonlinear behavior and higher uncertainty. This is suitable for both Λ and θ_p . For the former, this classification was made in view of the fact that the rate of cyclic deterioration is indicative of the actual ductility: Higher rates (lower Λ) mean less ductile steel sections.
- c) Brittle, ductility-based: This is the case for the ultimate rotation of the member hinges that corresponds to fracture. Fracture due to low-cycle fatigue is strongly linked to θ_{pc} in the sense that the latter controls how fast a structural component buckles locally and consequently affects its failure rate.

Table 1 summarizes the values suggested by FEMA P-58-1 [20] for the description of the three different failure mode types.

Table 1. Dispersion values proposed by FEMA P-58-1 [20] for the uncertainty components. The material is assumed to be any steel grade other than ASTM A36.

Damage-State type	Design equation	Material	Construction quality, β_C		
			Good	Average	Low
ductile, simple	β_D	β_M	0	0	0
ductile, complex	0.05	0.1	0	0.15	0.25
brittle, ductility-based	0.10	0.1	0	0.15	0.25
	0.25	0.1	0	0.15	0.25

Table 2. Dispersion values for the hinge properties of the steel frame as per Lignos & Krawinkler [17] and FEMA P-58 [20]. The reported parameter is the coefficient of variation for normal variables and the (closely related) standard deviation of the log data for lognormal distributions.

Quality	Member type	θ_p^1	θ_{pc}^1	Λ^1	$M_y/M_{y,p}^2$	M_c/M_y^2
good	Beam	0.24	0.26	0.35	0.12	0.03
	Column	0.35	0.24	0.34	0.21	0.05
average	Beam	0.28	0.30	0.38	0.12	0.03
	Column	0.38	0.28	0.37	0.21	0.05
low	Beam	0.35	0.36	0.43	0.12	0.03
	Column	0.43	0.35	0.42	0.21	0.05

¹ lognormal ² normal

Since the FEMA P-58 recommendations are only a generic process to be applied whenever sufficient data is not available, we have chosen to use it instead only to extend the usefulness of the Lignos & Krawinkler [17] dataset. Thus, as their findings mostly correspond to laboratory-quality specimens, rather than actual connections from the field, they are

considered to correspond to the top quality rating, i.e., “very good” (henceforth referred to as simply “good”). Hence, in terms of Eq. (1), the reported dispersions are taken to fully account for the effect of the β_D , β_M and β_{min} (i.e. $\beta_{Lignos\&Krawinkler} = \sqrt{\beta_D^2 + \beta_M^2 + \beta_{min}^2}$). Then, the effect of lesser construction qualities was added by also including the β_C term (i.e. $\beta = \sqrt{\beta_{Lignos\&Krawinkler}^2 + \beta_C^2} \leq \beta_{max}$) and disregarding any potential cutoff by the (only suggested after all) value of β_{max} (Table 2).

Table 3. Random variables correlation coefficients for beams and columns.

Beams	θ_p	θ_{pc}	Λ	$M_y/M_{y,p}$	M_c/M_y
	1	0.54	0.65	0	0
	0.54	1	0.63	0	0
	0.65	0.63	1	0	0
	0	0	0	1	0
	0	0	0	0	1
Columns	θ_p	θ_{pc}	Λ	$M_y/M_{y,p}$	M_c/M_y
	1	0.60	0.56	0	0
	0.60	1	0.58	0	0
	0.56	0.58	1	0	0
	0	0	0	1	0
	0	0	0	0	1

For a spatial probabilistic model, two types of variable correlation need to be accounted for, namely intra- and inter-component. Intra-component correlation connects the probabilistic properties of parameters within the same hinge, and it can be derived from the statistical treatment of connection test results. Each property (θ_p , θ_{pc} etc) of the hinge shares the same spatial correlation structure, regardless of its distribution type. In the particular case of rotational capacities, the marginal distributions are lognormal, therefore the overall distribution becomes a multivariable joint lognormal. Corresponding correlation values for each of the five hinge parameters are reported in Table 3 [17; 31]. Inter-component correlation essentially reflects the spatial distribution of the parameters throughout the structure, being dependent on the consistency in workmanship and material quality among different members, sections and connections. Its assessment is quite difficult, as it requires extensive data from actual structures, which are obviously scarce. In our opinion, the best, if not the only, data so far have been provided by Idota et al [32] who actually tested coupons from each production lot of steel members and then tracked them to their actual positions in a six-story six-bay steel frame. They suggested a correlation coefficient of 0.65 for the yield strength of beams or columns belonging to the same production lot. Due to the small size of our four-story two-bay frame, this value was taken to characterize all plastic hinges in members of the same section. Thus, relatively high inter-component correlations exist among beams at stories 1-2 and 3-4 (see Fig. 1). Similarly for the columns, US construction practice dictates that a single member typically crosses two stories until a splice occurrence at mid-story to change to a new section. Thus, as each column line of ~15.5m height is essentially composed of two members of different section spliced at the middle of the 3rd floor, column plastic hinges are well correlated above and then below the splice (Fig. 1). Generally speaking, it is not a trivial task to assess *a priori* what would have been the effect of adopting a higher or a lower inter-component correlation coefficient on the building’s seismic performance. Idota et al [32] for a single mid-rise frame, reported for lower correlation coefficients slightly lower ultimate frame strengths as well as a reduced variation, but this might not to be a general trend. To this end, inter-component correlation coefficient is

anticipated to have a small impact in relatively small buildings but more caution should be exercised when selecting such a property for larger buildings, where the likelihood of the same sections belonging to different production lots is much higher. Obviously, the aforementioned observations are founded on the assumption that the steel manufacturer operates under internationally accepted quality control standards.

3 PERFORMANCE ASSESSMENT

3.1 Methodology

Incremental Dynamic Analysis (IDA) is employed to determine the seismic response of the model structure for various combinations of the uncertain parameters. IDA [21] is a powerful analysis method that involves performing a series of nonlinear response history analyses for a suite of ground motion records scaled at increasing intensity levels. To define IDA curves of seismic intensity versus response, two scalars are needed, these being an intensity measure (IM) to represent the seismic intensity and an engineering demand parameter (EDP) to record the structural response. For the present study the 5% damped first-mode spectral acceleration $S_a(T_1, 5\%)$ is used as the IM whereas, the peak story drifts for the individual i -stories θ_i , the maximum interstory drift θ_{max} and the peak roof drift θ_{roof} are used as EDPs.

To account for the uncertainties induced by the random parameters to the structural system, IDA is paired with Monte Carlo simulation that employs efficient incremental record-wise Latin Hypercube Sampling (LHS) [22] to propagate the uncertainties from the numerous parameters to the actual system demand and capacity. Whereas usually a full record suite is used to analyze each model sample, this approach undertakes LHS simultaneously on the structural properties and the seismic input to achieve considerable savings. Hence, instead of maintaining the same model realization and analyzing it over the entire suite of ground motions, the latter also becomes a random variable in the sense that each model realization (or each set of structural properties) is paired to a single different ground motion that is also randomly selected from a bin of records. Furthermore, the adopted LHS conducts an incremental convergence process whereby only ten SMRF realizations (each one analyzed for one record) are used in the first iteration and then, for each subsequent cycle, sample size is doubled by adding first 10 and then 20, 40, 80, 160 new observations to reach a total of 320. Such new SMRF realizations are defined in such a way that they form a proper latin hypercube together with the already analyzed sample, thus minimizing waste [22]. A typical LHS application in such a setting would necessitate a far larger number of analyses, simply because of not knowing a priori what size to choose.

The analyses for each construction quality level involved a total of 200 random variables and 60 “ordinary” ground motion records (i.e. without any soft soil or directivity issues). The records were recorded on firm soil sites and selected from a relatively narrow magnitude and distance band. Hence, their moment magnitude ranges from 6.5-6.7 whereas their closest distance to the fault rupture varies within 13.3-31.7km [33]. Furthermore, high scale factors were involved. It should be mentioned though, that record selection and scaling and any sufficiency issues that might be raised by such choices are not important in the present study, since we are not convolving the results with the seismic hazard. Hence, any potential bias induced to the final product of a probabilistic analysis (i.e. mean annual frequency of exceeding a limit state) by such choices is irrelevant to this study and won’t affect the comparative results presented. For the abovementioned reason our discussion is not focused on the record selection as well as on issues relative to sufficiency. As previously discussed, the record-wise LHS design was applied with a starting size of 10 that was incrementally increased over 6 generations to a maximum sample of 320. Actually, only 4 to 5 generations

at 80 to 160 samples respectively, are sufficient in order to achieve fairly stable response estimates, regardless of the level of dispersion (i.e. construction quality) assumed. After the fourth generation, the relative errors in the median and dispersion in S_a differ only slightly, irrespectively of the considered EDPs and the limit (or damage) states.

3.2 Global damage-states: Deformation-based

Figure 3a illustrates the IDA curves for ‘good’ construction quality. It is apparent that the record-to-record variability is fairly large especially at high interstory drift demands where the building is approaching collapse. These results can be further summarized into 16,50,84% fractile IDA curves, that are presented in Figure 3b. As illustrated, given for instance a $S_a(T_1,5\%)$ of 1.0g, 16% of the samples produce approximately a $\theta_{max} \leq 3\%$, 50% of the samples a $\theta_{max} \leq 4.5\%$ and 84% of the samples a $\theta_{max} \leq 10\%$.

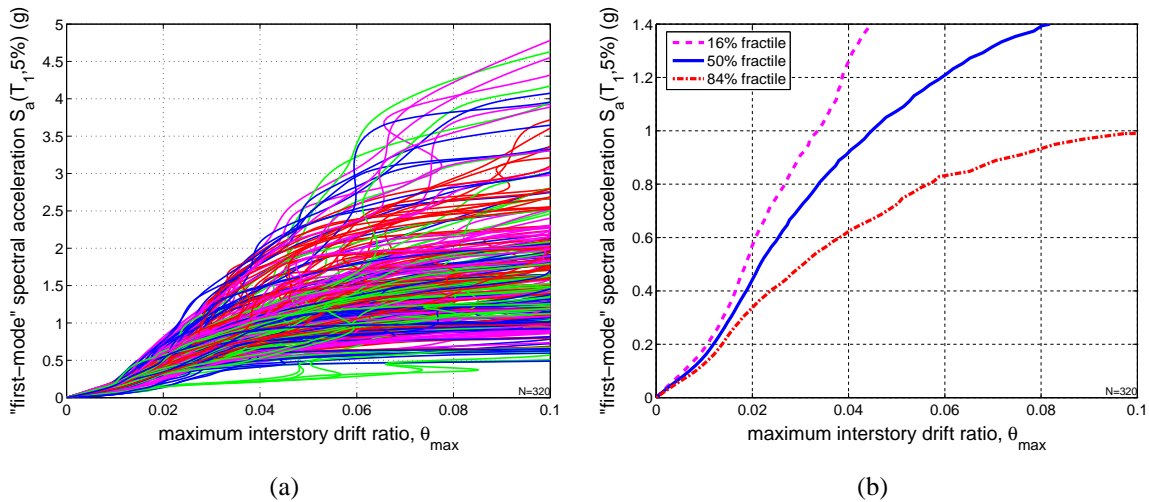


Figure 3. (a) 320 IDA curves and (b) 16, 50, 84% fractile values (‘good’ construction quality).

The extent to which the model parameters affect the seismic performance of the analyzed building can be revealed via comparison studies of the median IDAs and dispersions obtained considering the uncertainty in the structural parameters of the modeled structure (generation 6 with $N=320$) and a deterministic mean-parameter model. The term “mean-parameter” refers to the typical engineering approach where parameter uncertainty is disregarded by setting all properties to their mean value. In that case, only the record-to-record variability is considered by using the 60 ground motion records. As illustrated in Figure 4, for the ‘good’ construction quality, the evaluated medians and dispersions of S_a capacities given the maximum interstory drift ratio θ_{max} are almost identical (Fig. 4a and 4b). In other words, any bias and variance introduced by the parameter uncertainty appear to be very limited. Furthermore, the results were found to differ only marginally for other EDPs, i.e. the individual story drifts θ_i , the peak roof drift θ_{roof} or any of the lesser quality levels.

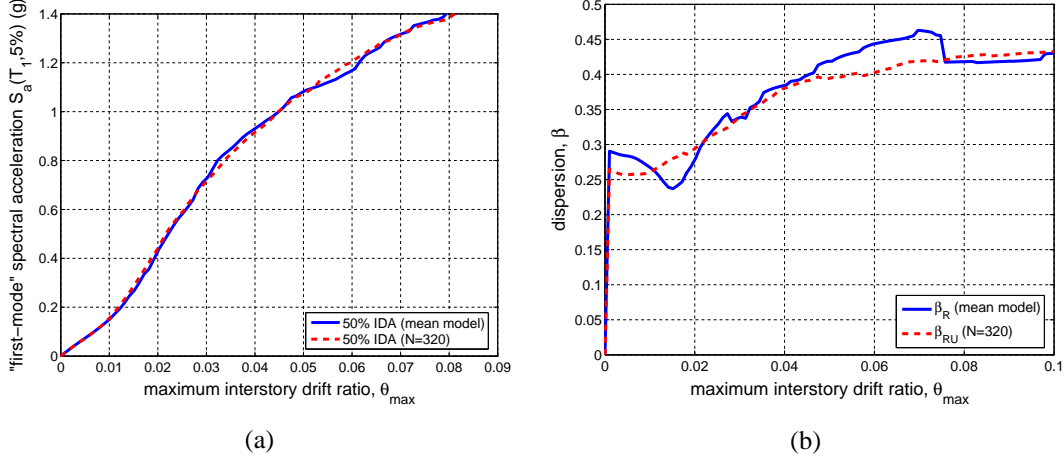


Figure 4. Record wise vs. mean model median IDAs and S_a capacity dispersions for ‘good’ construction quality level.

Hence, given the remarkable agreement between the mean-parameter and the computationally expensive uncertain model it can be said that, at least for the case of a low-rise capacity-designed SMRF, the model parameter uncertainty effect may be safely ignored. These observations further support findings in previous studies (e.g. [11; 14]), which suggested that the uncertainty associated to the acceleration “signature” is so significant that it dominates over any variability associated to the structural properties, at least for capacity-designed buildings away from their global collapse state. By contrast, for a regular nine-story SMRF studied by Vamvatsikos & Fragiadakis [9] the median collapse capacity was found to be moderately lowered by the uncertainty associated with the ultimate ductility. In the present study though, this was not observed since any significant influence of the ultimate ductility was cancelled out by the cyclic degradation, a hysteretic property that was disregarded before by Vamvatsikos & Fragiadakis [9]. Hence, at least for the case considered, cyclic degradation was found to have a more symmetric effect, meaning that lowering or increasing the parameter Λ does influence similarly the structural response. However, this finding remains to be further verified for other structural configurations. In general though, it can be said that, a global damage state assessment via a deformation-based global demand parameter won’t be affected much by the model parameter uncertainties. Instead, when performing loss assessment, seemingly identical components (same floor, same demand, same size), are anticipated to sustain different levels of damage due to uncertainty.

3.3 Local damage-states: Demand-capacity correlation

Whereas story-level responses, e.g. θ_{max} , were utilized so far to define building damage-states, we shall now look at seismic fragility in finer detail by moving to the component-level to consider local damage-states. Fragility is defined as the probability function of the limit-state capacity C being exceeded by the demand D for a given intensity level (i.e. IM-value), s . If demand and capacity are expressed in terms of intensity levels, then we get the simplest representation of fragility:

$$P_{LS}(s) = P(C < D | s) = P(s_c < s | s) = F(s_c | s) \quad (2)$$

where, s_c is the (random) IM-value of capacity that when exceeded signals violation of the limit-state and $F[\cdot]$ is the cumulative distribution function (CDF) of its arguments. Essentially, the fragility curve is the CDF of s_c evaluated at the intensity level s . Under the typical lognormal distribution assumption for s_c the following well-known expression appears:

$$P_{LS}(s) = \Phi\left(\frac{\ln s - \ln \hat{s}_c}{\beta_{Sc}}\right) \quad (3)$$

where, \hat{s}_c is the median IM-value of capacity and β_{Sc} the corresponding dispersion (i.e. standard deviation of the log data).

An equivalent, yet more intuitive, basis for defining fragility appears if both C and D from Eq. (2) are expressed in terms of EDPs: D is the local seismic demand for the component (e.g. plastic hinge rotation) while C is the corresponding capacity or threshold of component response whose exceedance defines the damage-state. Then, in the region away from global collapse where such a formulation is possible (see e.g., [34]) Eq. (2) becomes:

$$P_{LS}(s) = \Phi\left[\frac{\ln s - (\ln \hat{\theta}_c - \ln a) / b}{\beta_{T\theta} / b}\right] \quad (4)$$

where $\beta_{T\theta}$ is the overall dispersion in EDP terms due to demand and capacity variability, $\hat{\theta}_c$ is the median EDP capacity while the constants a and b are used to fit the median EDP response given s via a power law, or $\hat{\theta}(s) \approx a \cdot s^b$. Note that such building-level fragilities (which will be our focus) are entirely different from component-level fragility functions, typically used for detailed loss assessment (e.g., FEMA P-58). These are used to define component damage states given values of the EDP, rather than the IM, thus reverting to the simpler form of Eq. (3) but parameterized in terms of θ rather than s .

In either case, as both C and D are inherently random (typically lognormal) when expressed in terms of EDP, their potential correlation becomes an issue affecting both formulations (although not as apparent in the case of Eq. (3)). Formally,

$$\beta_{T\theta}^2 = \beta_{\theta d}^2 + \beta_{\theta c}^2 - 2\rho\beta_{\theta d}\beta_{\theta c} \quad (5)$$

where ρ is the correlation coefficient and $\beta_{\theta d}$, $\beta_{\theta c}$ the dispersion of D and C , respectively. Current literature typically adopts the hypothesis that the EDP demand and capacity are uncorrelated, or $\rho = 0$. This is a rational choice for a structural model with deterministic properties, but not necessarily so for an ‘uncertain’ structure. In the latter case DC correlation manifests itself in the sense that lower member capacities lead to higher structural demands and vice versa, thus factually linking local demands and capacities. Then, as suggested by Cornell et al [23] and adopted by the SAC/FEMA guidelines, a perfect negative correlation of $\rho = -1$ (at least for the epistemic component of dispersion) may make more sense. Still, its effect on the seismic risk assessment studies and whether it is significant for performance assessment has not been thoroughly examined. To the authors’ knowledge, only two studies that address the DC correlation issue have appeared, considering only reinforced concrete buildings. The first is by Jalayer et al [35], in which the critical DC ratio, associated to the component that leads the system close to failure, was adopted as an EDP. For the considered generic 8-story reinforced concrete building, the DC correlation was found to inflate the fragility dispersion. The second is the work of Dolsek [36] who evaluated the seismic risk of a 4-story concrete building considering limit states that were paired to the modeled plastic hinge properties. The risk for ‘near collapse’ was found to be more than twice as high when considering DC correlation.

On account of the above, the importance of DC correlation will be evaluated for the 4-story SMRF for the three considered construction quality levels on three different premises:

- a) Case 0, Mean model, no uncertainty and no DC correlation: Deterministic mean-parameter model analyzed by considering only record-to-record variability (60 records) where the exceedance of the limit state is checked by comparing the local

demands for each record sample to the mean rotational capacity of each individual hinge. This is the typical assessment case.

- b) Case 1, Uncertainty and no DC correlation: 320 random building-record pairs where the exceedance of the limit state is checked in each building-record sample by comparing the local demands to the mean rotational capacity of each individual hinge.
- c) Case 2, Uncertainty and full DC correlation: 320 random building-record pairs where the exceedance of the limit state is checked in each building-record sample by comparing the local demands to the actual random rotational capacity of each individual hinge.

For all three cases, two damage/limit states are considered. The first is Local Damage, associated to the first exceedance of the capping rotation capacity (i.e. initiation of negative stiffness) at the end of any structural element (beam or column), θ_p . This is considered sufficient to undermine the life safety of the building' occupants and hence may be assumed to be roughly analogue to the Life Safety (LS) performance objective as per FEMA 350 [26]. The second is Local Failure, linked to a near-fracture of a plastic hinge and determined by the first exceedance of an adjusted ultimate plastic hinge rotation. Originally, the backbone of Figure 2 would suggest a local failure rotation of $\min(\theta_u, \theta_p + \theta_{pc})$. Still, this would disregard the influence of cyclic degradation that may rapidly lower the moment strength of the hinge through the uncertain parameter Λ . Optimally one would keep track of both rotation and moment at the hinge and use both to determine a significant permanent loss of capacity. The reason is that hinge fracture depends on the loading history that the component is subjected as part of a structure (e.g. near fault versus long duration earthquake) [37]. In lieu of this we propose a simple rotation-only criterion that approximately checks for a 50% loss in moment capacity assuming that previous inelastic cycles have already accounted for a $5\theta_p M_y$ hysteretic energy (in the order of a full cycle of deformation within $+\theta_p$ and $-\theta_p$). For our purposes, the exact level of previously dissipated energy is not important as long as it is large enough to allow the manifestation of deterioration. Experimental data would help with finding a consensus value for wider application. In the case at hand, using the appropriate degradation rule [17] the limiting rotation value becomes $\theta_{lim} = \theta_p + \max(0.5 - 5\theta_p/\Lambda, 0) \cdot \theta_{pc}$.

The effect of each modeling choice is shown in Table 4, which contains the statistics of the median and dispersion of the spectral acceleration capacity, s_c , while Figure 5 illustrates the fragility curves themselves. Evidently, the two damage-states are affected in a similar but not identical way. For Local Damage in particular, the introduction of uncertainty and DC correlation reduces the median capacity and also increases the dispersion by as much as 15%. The reduction associated with the median is shown in Figures 5a,b as a characteristic left-shift of the fragility curves, which for the low construction quality level is approximately 17%. This is actually in spite of the relatively high values of correlation used and the small number of elements in each story. Larger buildings and less correlated elements would easily see larger changes, simply due to the higher chance of one of the many uncertain elements hitting exceedance first (as befitting a series system in reliability terms). Notably, the observed results clearly violate the first-order assumption (e.g., Cornell et al [23]) that uncertainty does not impact the median but only the dispersion. Even when uncertainty is modeled as non-biasing at the parameter level (as done herein), its effect can affect the mean/median when propagated to the system response.

Table 4. Median and dispersion of the spectral acceleration capacity for three levels of construction quality and two damage-states, local damage and local failure, corresponding to exceedance of θ_p and θ_{lim} , respectively. For comparison, the mean model fragility values are also shown.

Construction quality	Cases	Local Damage		Local Failure	
		\hat{s}_c	β_{Sc}	\hat{s}_c	β_{Sc}
mean model	Case 0	0.65	0.31	1.25	0.38
good	Case 1	0.65	0.32	1.29	0.42
	Case 2	0.58	0.34	1.22	0.44
average	Case 1	0.64	0.31	1.23	0.39
	Case 2	0.57	0.36	1.17	0.38
low	Case 1	0.63	0.31	1.29	0.39
	Case 2	0.54	0.35	1.15	0.41

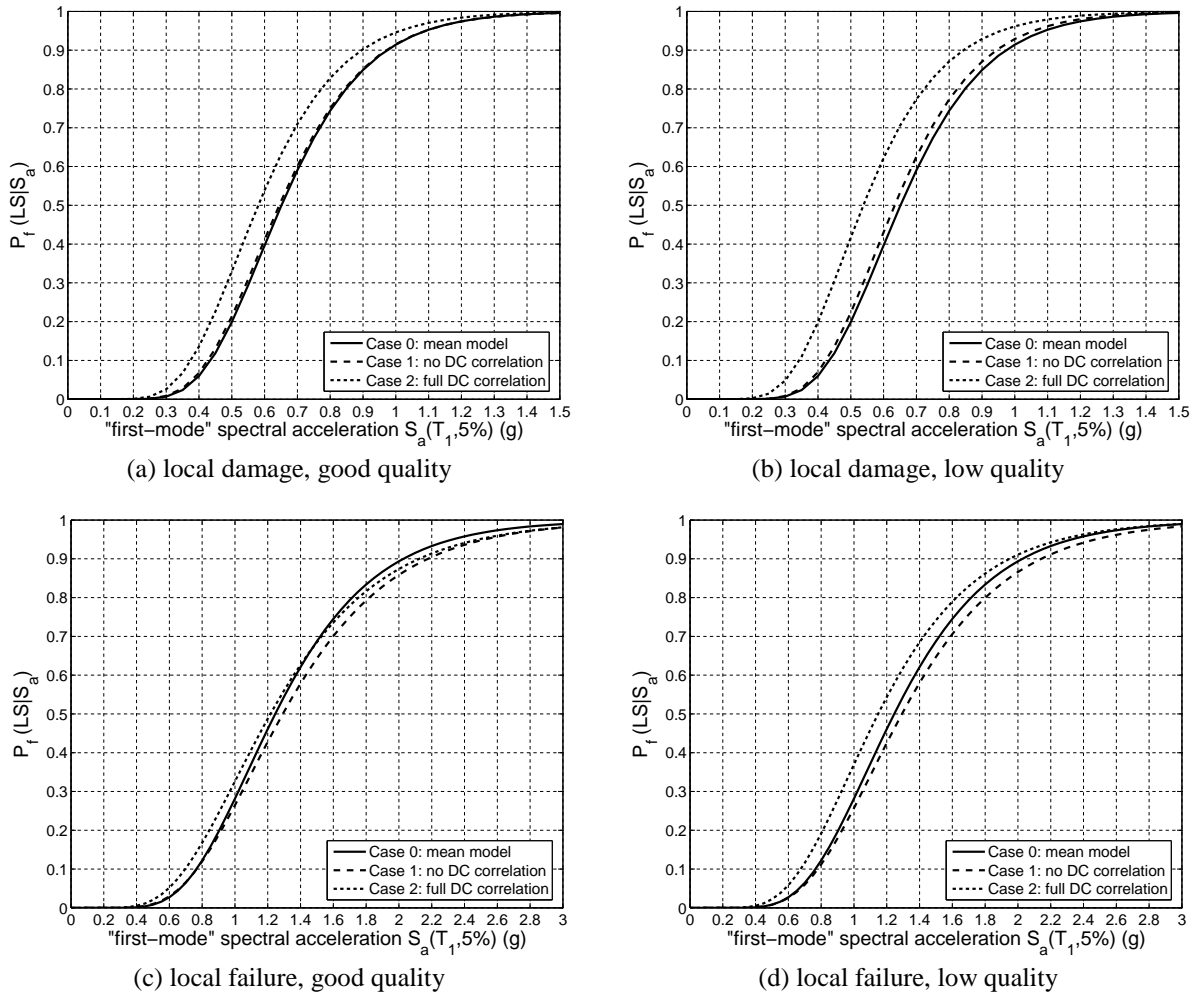


Figure 5. The effect of uncertainty and DC correlation on fragility curves for different damage-states and construction qualities. It mainly appears as decrease (bias) of the median S_a required to exceed θ_p (local damage) and θ_{lim} (local failure).

For encountering Local Failure, the introduction of uncertainty along with the DC correlation (i.e. Case 2) also reduces the median, but to a lesser extent compared to the Local Damage state whereas, the dispersion is generally increased. The lower changes in the median can be attributed to the relative proximity of this limit-state to global collapse for this small-size structure. There is not enough margin of seismic intensity between the first and the last

hinge failure. Thus, the appearance of the flatline in terms of IDA (which we have shown to be quasi-insensitive to such local issues for this building) tends to dampen the effects of an early failure. This becomes apparent when one considers the model parameter uncertainties but disregards DC correlation (i.e. Case 1). Then the median capacity s_c even seems to be slightly higher for the good and the low construction qualities compared to that evaluated on a mean model basis (i.e. Case 0). The aforementioned findings appear in Figures 5c,d as a right-shift of Case 1 fragilities compared to the expected left-shift of Case 2 fragilities. The former is not a statistically significant difference: It that should be interpreted as Case 1 not being appreciably different from Case 0 for Local Failure. Hence, it can be generally said that the bias induced to the capacity estimates, when considering limit state exceedance at a local level, either via disregarding the model parameter uncertainties or by not considering the DC correlation, could well lead to non conservative fragility estimates. Furthermore, for the sole building investigated in this research study, the induced bias in the median capacity estimates was found to increase for lower construction quality control levels.

Eq. (5) can help us understand the observed synergy between uncertainty and DC correlation: When ρ is close to -1 [23] the total dispersion is increased by $2\beta_{\theta_c}\beta_{\theta_d}$. If the effect of uncertainty, mainly expressed by β_{θ_c} (although β_{θ_d} is also influenced but to a smaller degree), is sizeable enough, then the DC correlation term will immediately become significant as well. Otherwise, its effect disappears together with the low effect of the parameter uncertainty.

4 CONCLUDING DISCUSSION

An accurate quantification of the model parameter uncertainty effects on the seismic performance has been presented for a 4-story steel moment-resisting frame designed for Western USA. The comparison of the interstory drifts obtained with and without the consideration of model parameter uncertainties revealed that their effect can be safely ignored for the examined case, i.e., for regular low-rise capacity-designed steel frame buildings, as long as one is interested in the global behavior. This conclusion actually stands regardless of the construction quality control that is exercised during construction (assuming no gross errors occur of course). Nevertheless, when it comes to local component damage, or loss assessment, the negative correlation of the uncertain local structural demands and member capacities (where higher demands generally correspond to weakened members) is likely to give rise to unconservative estimates: While the dispersion of the associated fragility is not much influenced, the median intensity required to cause local exceedance of a damage-state is reduced compared to that evaluated on the basis of the mean model. This reduction was found to be more severe for damage-states away from the global collapse state and for low construction quality levels. Nevertheless, it is suspected that such effects may rise in importance for buildings vulnerable to localized modes of failure, such as a story-mechanism. This is the case of, e.g. older non-capacity-designed structures, or even modern steel buildings with braced frames as their primary lateral load resisting system. Still, further research is needed before a proper assessment can be made.

ACKNOWLEDGEMENT

This work has been supported by the European Research Executive Agency via Marie Curie grant PCIG09-GA-2011-293855 and co-financed by Greece and the European Union (European Social Fund) through the Operational Program “Human Resources Development” of the National Strategic Framework (NSRF) 2007-2013. The authors also wish to acknowledge the help they received from the anonymous reviewers with improving the manuscript.

REFERENCES

1. Wen YK, Ellingwood BR, Veneziano D and Bracci J. 2003. Uncertainty Modeling in Earthquake Engineering. MAE Center Project FD-2 Report.
2. Kwon OS and Elnashai A. The effect of material and ground motion uncertainty on the seismic vulnerability curves of RC structure. *Engineering Structures* 2006; **28**(2): 289–303.
3. Kazantzi AK, Righiniotis TD and Chryssanthopoulos MK. Fragility and hazard analysis of a welded steel moment resisting frame. *Journal of Earthquake Engineering* 2008; **12**(4): 596–615.
4. Jeong SH and Elnashai AS. Probabilistic fragility analysis parameterized by fundamental response quantities. *Engineering Structures* 2007; **29**(6): 1238–1251.
5. Dolsek M. Incremental dynamic analysis with consideration of modelling uncertainties. *Earthquake Engineering and Structural Dynamics* 2009; **38**(6): 805–825.
6. Liel AB, Haselton CB, Deierlein GG and Baker JW. Incorporating modeling uncertainties in the assessment of seismic collapse risk of buildings. *Structural Safety* 2009; **31**(2): 197–211.
7. Jalayer F, Iervolino I and Manfredi G. Structural modeling uncertainties and their influence on seismic assessment of existing RC structures. *Structural Safety* 2010; **32**(3): 220–228.
8. Franchin P, Pinto PE and Rajeev P. Confidence factor? *Journal of Earthquake Engineering* 2010; **14**(7): 989–1007.
9. Vamvatsikos D and Fragiadakis M. Incremental dynamic analysis for estimating seismic performance sensitivity and uncertainty. *Earthquake Engineering and Structural Dynamics* 2010; **39**(2): 141–406.
10. Ibarra L and Krawinkler H. Variance of collapse capacity of SDOF systems under earthquake excitations. *Earthquake Engineering and Structural Dynamics* 2011; **40**: 1299–1314.
11. Kazantzi AK, Righiniotis TD and Chryssanthopoulos MK. A simplified fragility methodology for regular steel MRFs. *Journal of Earthquake Engineering* 2011; **15**(3): 390–403.
12. Luco N and Cornell CA, 1998. Effects of random connection fractures on the demands and reliability for a 3-story pre-Northridge SMRF structure. Proceedings of the 6th U.S. National Conference on Earthquake Engineering, Seattle, Washington.
13. Song J and Ellingwood BR. Seismic reliability of special moment steel frames with welded connections: II. *Journal of Structural Engineering (ASCE)* 1999; **125**(4): 372–384.
14. Kazantzi AK, Righiniotis TD and Chryssanthopoulos MK. The effect of joint ductility on the seismic fragility of a regular moment resisting steel frame designed to EC8 provisions, *Journal of Constructional Steel Research* 2008; **64**(9): 987–996.
15. FEMA 355D, 2000. State of the art report on connection performance, prepared by Federal Emergency Management Agency, Washington, DC.
16. Mele E. Moment resisting welded connections: An extensive review of design practice and experimental research in USA, Japan and Europe. *Journal of Earthquake Engineering* 2002; **6**(1): 111–145.
17. Lignos DG and Krawinkler H. Deterioration modeling of steel components in support of collapse prediction of steel moment frames under earthquake loading. *Journal of Structural Engineering (ASCE)* 2011; **137**(11): 1291–1302.
18. Lignos DG and Krawinkler H. Development and utilization of structural component databases for performance-based earthquake engineering. *Journal of Structural Engineering (ASCE)* 2013; **139**(NEES 2): 1382–1394.

19. Fragiadakis M, Vamvatsikos D and Papadrakakis M. Evaluation of the influence of vertical irregularities on the seismic performance of a 9-storey steel frame. *Earthquake Engineering and Structural Dynamics* 2006; **35**(12): 1489–1509.
20. FEMA, 2012. Seismic performance assessment of buildings, Volume 1-Methodology, FEMA P-58-1, prepared by the Applied Technology Council for the Federal Emergency Management Agency, Washington, DC.
21. Vamvatsikos D and Cornell CA. Incremental dynamic analysis. *Earthquake Engineering and Structural Dynamics* 2002; **31**(3): 491–514.
22. Vamvatsikos D. Seismic performance uncertainty estimation via IDA with progressive accelerogram-wise Latin Hypercube Sampling. *Journal of Structural Engineering* 2014; [http://dx.doi.org/10.1061/\(ASCE\)ST.1943-541X.0001030](http://dx.doi.org/10.1061/(ASCE)ST.1943-541X.0001030).
23. Cornell CA, Jalayer F, Hamburger RO and Foutch DA. Probabilistic basis for 2000 SAC Federal Emergency Management Agency steel moment frame guidelines. *Journal of Structural Engineering* 2002; **128**(4): 526–533.
24. IBC, 2003. International building code IBC 2003, International Code Council, Birmingham, AL.
25. AISC, 2005. Seismic provisions for structural steel buildings, including supplement No. 1, American Institute of Steel Construction, Inc. Chicago, Illinois.
26. FEMA 350, 2000. Recommended seismic design criteria for new steel moment frame buildings, prepared by Federal Emergency Management Agency, Washington, DC.
27. McKenna F, Fenves G, Jeremic B and Scott M, 2000. Open system for earthquake engineering simulation. <<http://opensees.berkeley.edu>> (Nov. 1, 2013).
28. Gupta A, Krawinkler H, 1999. Seismic demands for performance evaluation of steel moment resisting frame structures. Rep. No. 132, The John A. Blume Earthquake Engineering Center, Stanford Univ., Stanford, CA.
29. Lignos DG, Krawinkler H and Whittaker AS. Prediction and validation of sidesway collapse of two scale models of a 4-story steel moment frame. *Earthquake Engineering and Structural Dynamics* 2011; **40**(7): 807–825.
30. Ibarra LF, Medina RA and Krawinkler H. Hysteretic models that incorporate strength and stiffness deterioration. *Earthquake Engineering and Structural Dynamics* 2005; **34**(12): 1489–1511.
31. Lignos DG and Krawinkler H, 2012. Sidesway collapse of deteriorating structural systems under seismic excitations. Rep. No. TB 177, The John A. Blume Earthquake Engineering Center, Stanford Univ., Stanford, CA.
32. Idota H, Guan L and Yamazaki K, 2009. Statistical correlation of steel members for system reliability analysis. Proceedings of the 9th International Conference on Structural Safety and Reliability (ICOSSAR), Osaka, Japan.
33. Vamvatsikos D and Sigalas I, 2005. Seismic performance evaluation of a horizontally curved highway bridge using incremental dynamic analysis in 3D. Proceedings of the 4th European Workshop on the seismic behaviour of irregular and complex structures, Thessaloniki, Greece.
34. Vamvatsikos D. Derivation of new SAC/FEMA performance evaluation solutions with second-order hazard approximation. *Earthquake Engineering and Structural Dynamics* 2013; **42**(8): 1171–1188.
35. Jalayer F, Franchin P and Pinto PE. A scalar decision variable for seismic reliability analysis of RC frames. *Special issue of Earthquake Engineering and Structural Dynamics on Structural Reliability* 2007; **36**(13): 2050–2079.
36. Dolsek M. Simplified method for seismic risk assessment of buildings with consideration of aleatory and epistemic uncertainty. *Structure and Infrastructure Engineering* 2011; **8**(10): 939–953.

37. Lignos DG, Chung Y-L, Nagee T and Nakashima M. Numerical and experimental evaluation of seismic capacity of high-rise steel buildings subjected to long duration earthquakes. *Journal of Computers and Structures* 2011; **89**(11-12): 959–967.